

## A NOVEL FIELD SCATTERING FORMULATION FOR POLARIMETRIC SYNTHETIC APERTURE RADAR: 3D SCATTERING AND STOKES VECTORS

Ramin Sabry\*

Radar Application & Space Technology, Defence R&D Canada, 3701 Carling Avenue, Ottawa, Ontario K1A 0Z4, Canada

**Abstract**—Conventional Far-field decomposition of the scattered electromagnetic (EM) field in the  $[EH]$  plane in terms of the horizontal and vertical components (i.e.,  $h$ ,  $v$ ), introduces ambiguity for multi-static, multi-platform and/or scene-centric polarimetric synthetic aperture radar (SAR) image exploitation. This is due to the fact that a 2-dimensional (2D) vector field can not constitute a complete space capable of modeling 3-dimensional (3D) field transformations. To address this, analytic extension of the Stokes and scattering vectors to 3D is explored and presented. In particular, coherent 3D polarimetric decomposition in Gell-Mann basis is introduced and explored as 3D generalization of standard Pauli decomposition. The results are also applicable to compact polarimetry (CP) where mathematically consistent 3D Stokes parameters can be defined.

### 1. INTRODUCTION

Synthetic aperture radar (SAR) and radar polarimetry literature contain a wide variety of target classification and decomposition techniques based on electromagnetic (EM) scattering theory using incoherent and coherent methods and products [1–10]. Scattering functions (e.g., scattering matrix, EM field vectors) provide a reasonable measure and data set for single platform SAR exploitation, i.e., single line of sight (LOS) backscattering. 2-dimensional (2D) backscattering observations and scattering matrix derivations provide complete information (Poynting's theorem under far-field assumption) for target or image exploitation in such cases that can apply observation-centric coordinate systems, i.e., unique  $h$ ,  $v$  transmission/reception. For scene-centric (coordinate system defined

---

*Received 19 June 2012, Accepted 9 November 2012, Scheduled 24 November 2012*

\* Corresponding author: Ramin Sabry (Ramin.Sabry@drdc-rddc.gc.ca).

at the scene center) and multi-platform (multi-LOS) SAR image exploitation, however, 2D formalism based on  $h$ ,  $v$  transmission and reception would not be straightforward. Furthermore, SAR operation and related image exploitation is not always guaranteed to be within targets' far field zone (e.g., near field SARs) that would make the field polarization more complicated. Such near field treatments and corrections has been applied for image processing [11], e.g., noise radar [20, 21] and some airborne scenarios [22]. Although radiometric aspects and corrections have been considered for similar problems, field polarization implications need to be investigated.

To remove the ambiguity that arises from the difference in 2D slicing of scattering (i.e., scattering planes) and harmonize scattering analysis to address the aforementioned limitations, it would be reasonable to formalize the analysis within a 3D framework. The end products can then be projected to or re-gauged for the desired 2D scattering plane without loss of consistency. The 3D framework is established here. It is shown that the formalism is consistent (e.g., unitary transformation, energy conservation) and can model a general partially polarized field in 3D when needed. A 2D picture that may be sufficient for majority of cases (though not practical for multi-LOS back/multistatic-scattering) can be found by proper reduction or re-gauging of the 3D picture. Application to compact polarimetry (CP) is also explored within the described 3D framework that allows introduction of mathematically consistent and universal scattering field observables (e.g., 3D Stokes parameters).

## 2. IMPORTANCE OF A 3D FIELD FORMALISM

For a scattering scenario that the EM field is assumed to be three dimensional (e.g., near field SAR) and/or measurable as such, the need for a 3D formalism is evident. Although this capability may currently exist for some ad-hoc applications (e.g., near field imaging) or be developed in future, the present discussion is mainly tailored and based on far field assumptions and current operational SARs. One should also note that present discussion is based on the 3D characteristics of the actual EM field and not what is conventionally measured, e.g., far-field power measurement. For a number of operational examples involving multistatic (multiple source/multi-LOS) scenarios, distributed targets, propagation media effects, and near-field scattering, the 2D EM field plane (or LOS) becomes ambiguous and/or incomplete. This shortcoming, in turn, introduces difficulty in inverse scattering solution, polarimetric SAR imaging and ensued exploitations. It will be shown that the 3D formalism of EM

field is invariant under transformation in a 3D space where the 2D gauging of the same EM field is not. More particular scenarios are explored as following.

### 2.1. Near-field Considerations

The far field zone of a target with mean reflective extent (source equivalent) of  $L$  can be estimated by  $r_{far} \approx 2\frac{L^2}{\lambda}$  [19] where  $\lambda$  is the operating wavelength. For a target length of  $L = 100$  m and X-band SAR imaging, the far field zone is defined at  $r_{far} \approx 800$  km. This limit is beyond operating range of airborne and some spaceborne SARs, even with conservative measures. Airborne SARs (e.g., Canada Convair-580) operate at a maximum altitude of 30,000 to 35000 ft (9.15 to 10.67 km). One of few and prominent fully polarimetric X-band SARs is DLR TerraSAR-X that circles earth in a polar orbit at 514 km altitude.

### 2.2. Multistatic Reception

Reception from multiple LOSs, e.g., multiple-transmit/multiple-receive, (in near or far field) underscores the non-uniqueness of a 2D  $[EH]$  plane defined at an observation point. Proper association or combination of multi-platform SAR polarimetric products can be made possible within a 3D framework. Analytic description of such 3D framework that can provide computational convenience and framework consistency is provided here. Polarimetric scattering products (e.g., matrices, vectors) from different platforms need to be expressed in a 3D format, transformed (using the introduced 3D transformations) to a reference/unique frame, and then be combined. If needed, the resulting final products can then be re-gauged to 2D for conventional or standard polarimetric analyses. Future spaceborne satellite missions such as RADARSAT Constellation Mission (RCM) combined with RADARSAT-2 (RS2) provide opportunities for multistatic target exploitation. A 3D approach can benefit the associated polarimetric data exploitation.

### 2.3. Compact Polarimetry

Compact polarimetry deals with imaging modes that transmit one polarization and coherently receive two orthogonal polarizations, neither of which matches the transmitted polarization. As such, Stokes vector and parameters that can characterize the partially-polarized scattered or receive EM field are suitable for required scattering analysis. The 2D Stokes 4-vector definition is specific to the assumed

LOS and respective  $[EH]$  plane. As will be shown analytically, any tilt of the assumed  $[EH]$  plane results in a different Stokes vector and associated parameters. While the corresponding transformation of 2D Stokes vector does not conserve energy, transformation of a 3D equivalent-to-Stokes vector (to be introduced) is unitary. Therefore, unique definition of the partially-polarized EM field Stokes observables can be provided using the 3D formalism.

### 3. ANALYTICAL FORMULATION

Consider a general 3D vector field:

$$\mathbf{E}(\mathbf{r}) = E_x \mathbf{x} + E_y \mathbf{y} + E_z \mathbf{z} \quad (1)$$

The associated field covariance matrix  $\mathbf{J}$  can be defined as:

$$\mathbf{J}^{(3D)} = \langle \mathbf{E} \mathbf{E}^\dagger \rangle = \begin{bmatrix} \langle |E_x|^2 \rangle & \langle E_x E_y^* \rangle & \langle E_x E_z^* \rangle \\ \langle E_y E_x^* \rangle & \langle |E_y|^2 \rangle & \langle E_y E_z^* \rangle \\ \langle E_z E_x^* \rangle & \langle E_z E_y^* \rangle & \langle |E_z|^2 \rangle \end{bmatrix} \quad (2)$$

where  $\langle \dots \rangle$  denotes temporal or local spatial averaging, and “ $\dagger$ ” represents the Hermitian conjugate. For remote sensing applications, scattering of the 3D field structure described by (1) and (2) need to be mathematically modelled by an equivalent 3D scattering matrix connecting the scattered to incident field, i.e.,  $3 \times 3$  scattering matrix instead of conventional  $2 \times 2$  scattering matrix as:

$$\mathbf{S}^{(3D)} = \begin{bmatrix} S_{xx} & S_{xy} & S_{xz} \\ S_{yx} & S_{yy} & S_{yz} \\ S_{zx} & S_{zy} & S_{zz} \end{bmatrix} \quad (3)$$

where  $\mathbf{E}^s(\mathbf{r}) = \mathbf{S}^{(3D)} \mathbf{E}^i(\mathbf{r})$ . Vectorization of the 3D scattering matrix  $V^{(3)}(\mathbf{S}^{(3D)})$  is performed in a similar manner as 2D scattering matrix vectorization  $V^{(2)}(\mathbf{S})$  [1]; the result is a 9-vector. The orthonormal eigenvector sets have covariance and coherency matrices,  $[C]_{9 \times 9}$  and  $[T]_{9 \times 9}$ , that share the same eigenvalues and form suitable basis sets for the vectorization of interest. The 3D scattering vector can then be expressed as:

$$\bar{\mathbf{S}}^{(3D)} = (S_{xx} \ S_{xy} \ S_{xz} \ S_{yx} \ S_{yy} \ S_{yz} \ S_{zx} \ S_{zy} \ S_{zz})^t \quad (4)$$

where “ $t$ ” denotes the transpose. The described commonality between Hermitian positive semi-definite covariance and coherency matrices (again, having the same set of eigenvalues) is provided through a unitary similarity transformation. For a 2D case, this transformation is established by four Pauli spin matrices (or vectors) in the form of:

$$A = \frac{1}{\sqrt{2}} \begin{bmatrix} 1 & 0 & 0 & 1 \\ 1 & 0 & 0 & -1 \\ 0 & 1 & 1 & 0 \\ 0 & -j & j & 0 \end{bmatrix} \quad (5)$$

Pauli decomposition (5) and respective mechanisms (e.g., single/double-bounce, volume) provide a complete description of scattering for 2D field ( $h, v$  basis) scenario, i.e., modeled by a  $2 \times 2$  matrix. Mathematically speaking, any  $2 \times 2$  scattering matrix can be expressed in Pauli basis. The 2D field scattering assumption is valid when far-field approximation that depends on target physics, distribution and observation specifications is satisfied (Poynting's theorem). However, if the scattered EM field is not completely represent-able within the EH plane at the observation point due to target and/or observation characteristics (e.g., target structure, near field operation), the  $2 \times 2$  scattering matrix representation cannot be complete. Hence, Pauli basis become incomplete and an extension to  $3 \times 3$  matrix basis set would be required. Such basis set capable of constructing a complete  $3 \times 3$  scattering matrix space can characterize any type of scattering including near-field due to the basis components' 3D nature, i.e., non-zero radial element. For a 3D scenario, the challenge is to seek a set of 9 orthogonal matrices or vectors constituting a 9-vector space. Considering the origins of Pauli spin matrices in quantum mechanics and their applications, use of the Gell-Mann matrices [12] to introduce the required transformation (similar to (5) for a 3D case) is proposed. There is, however, a difficulty associated with this: the Gell-Mann matrices [12] constitute eight matrices. Here, a ninth matrix (or vector) orthogonal to the set of eight Gell-Mann matrices is derived and added to the set of eight to derive the unitary transformation that is sought.

The orthonormal eight Gell-Mann matrices are:

$$\beta_1 = \frac{1}{\sqrt{2}} \begin{bmatrix} 0 & 1 & 0 \\ 1 & 0 & 0 \\ 0 & 0 & 0 \end{bmatrix} \quad (6)$$

$$\beta_2 = \frac{1}{\sqrt{2}} \begin{bmatrix} 0 & -j & 0 \\ j & 0 & 0 \\ 0 & 0 & 0 \end{bmatrix} \quad (7)$$

$$\beta_3 = \frac{1}{\sqrt{2}} \begin{bmatrix} 1 & 0 & 0 \\ 0 & -1 & 0 \\ 0 & 0 & 0 \end{bmatrix} \quad (8)$$

$$\beta_4 = \frac{1}{\sqrt{2}} \begin{bmatrix} 0 & 0 & 1 \\ 0 & 0 & 0 \\ 1 & 0 & 0 \end{bmatrix} \quad (9)$$

$$\beta_5 = \frac{1}{\sqrt{2}} \begin{bmatrix} 0 & 0 & -j \\ 0 & 0 & 0 \\ j & 0 & 0 \end{bmatrix} \quad (10)$$

$$\beta_6 = \frac{1}{\sqrt{2}} \begin{bmatrix} 0 & 0 & 0 \\ 0 & 0 & 1 \\ 0 & 1 & 0 \end{bmatrix} \quad (11)$$

$$\beta_7 = \frac{1}{\sqrt{2}} \begin{bmatrix} 0 & 0 & 0 \\ 0 & 0 & -j \\ 0 & j & 0 \end{bmatrix} \quad (12)$$

$$\beta_8 = \frac{1}{\sqrt{6}} \begin{bmatrix} 1 & 0 & 0 \\ 0 & 1 & 0 \\ 0 & 0 & -2 \end{bmatrix} \quad (13)$$

The complementary matrix is:

$$\beta_9^{(c)} = \frac{1}{\sqrt{3}} \begin{bmatrix} 1 & 0 & 0 \\ 0 & 1 & 0 \\ 0 & 0 & 1 \end{bmatrix} \quad (14)$$

Thus, the equivalent unitary similarity transformation ( $9 \times 9$ ) can be expressed as:

$$A^{(3D)} = \frac{1}{\sqrt{2}} \begin{bmatrix} \frac{\sqrt{6}}{3} & 1 & \frac{\sqrt{3}}{3} & 0 & 0 & 0 & 0 & 0 & 0 \\ 0 & 0 & 0 & 1 & 0 & 0 & -j & 0 & 0 \\ 0 & 0 & 0 & 0 & 1 & 0 & 0 & -j & 0 \\ 0 & 0 & 0 & 1 & 0 & 0 & j & 0 & 0 \\ \frac{\sqrt{6}}{3} & -1 & \frac{\sqrt{3}}{3} & 0 & 0 & 0 & 0 & 0 & 0 \\ 0 & 0 & 0 & 0 & 0 & 1 & 0 & 0 & -j \\ 0 & 0 & 0 & 0 & 1 & 0 & 0 & j & 0 \\ 0 & 0 & 0 & 0 & 0 & 1 & 0 & 0 & j \\ \frac{\sqrt{6}}{3} & 0 & -\frac{2\sqrt{3}}{3} & 0 & 0 & 0 & 0 & 0 & 0 \end{bmatrix}^t \quad (15)$$

Using (15), one can define the 3D target or scattering 9-vector in the Gell-Mann basis as:

$$k_{GM} = \frac{1}{\sqrt{2}} \begin{bmatrix} \frac{\sqrt{6}}{3} (S_{xx} + S_{yy} + S_{zz}) \\ S_{xx} - S_{yy} \\ \frac{\sqrt{3}}{3} (S_{xx} + S_{yy} - 2S_{zz}) \\ S_{xy} + S_{yx} \\ S_{xz} + S_{zx} \\ S_{yz} + S_{zy} \\ -j(S_{xy} - S_{yx}) \\ -j(S_{xz} - S_{zx}) \\ -j(S_{yz} - S_{zy}) \end{bmatrix} \quad (16)$$

As will be discussed, the coherent decomposition (16) can be viewed as 3D generalization of the conventional Pauli target decomposition. Similar to Pauli basis, the Gell-Mann basis matrices assume scattering by a perfect conductor. Considering the completeness of the Gell-Mann basis set that enables coherent decomposition of any complex  $3 \times 3$  scattering matrix, however, any scattering mechanisms can be mathematically modelled (similar to coherent decomposition of a general  $2 \times 2$  complex scattering matrix using Pauli basis). One can derive the 3D (9-vector) coherent EM field representation, i.e., equivalent-to-Stokes for 3D, as:

$$\overline{\overline{G}}_{(3D)} = \frac{1}{\sqrt{2}} \begin{bmatrix} \frac{\sqrt{6}}{3} \left( \langle |E_x|^2 \rangle + \langle |E_y|^2 \rangle + \langle |E_z|^2 \rangle \right) \\ \langle |E_x|^2 \rangle - \langle |E_y|^2 \rangle \\ \frac{\sqrt{3}}{3} \left( \langle |E_x|^2 \rangle + \langle |E_y|^2 \rangle - 2 \langle |E_z|^2 \rangle \right) \\ \langle E_x E_y^* \rangle + \langle E_y E_x^* \rangle \\ \langle E_x E_z^* \rangle + \langle E_z E_x^* \rangle \\ \langle E_y E_z^* \rangle + \langle E_z E_y^* \rangle \\ -j \left( \langle E_x E_y^* \rangle - \langle E_y E_x^* \rangle \right) \\ -j \left( \langle E_x E_z^* \rangle - \langle E_z E_x^* \rangle \right) \\ -j \left( \langle E_y E_z^* \rangle - \langle E_z E_y^* \rangle \right) \end{bmatrix} = \begin{bmatrix} W_0 \\ W_1 \\ W_2 \\ W_3 \\ W_4 \\ W_5 \\ W_6 \\ W_7 \\ W_8 \end{bmatrix} \quad (17)$$

It can be shown that for a completely depolarized wave, i.e.,  $E_x, E_y, E_z$  mutually incoherent and  $|E_x| = |E_y| = |E_z| = E$ :

$$W_1 = W_2 = W_3 = W_4 = W_5 = W_6 = W_7 = W_8 = 0 \quad (18)$$

and,

$$W_0 = \sqrt{3}E^2 \quad (19)$$

For a completely polarized wave that field components are mutually coherent, i.e.,  $\langle E_p E_q^* \rangle = E_p E_q^*, \forall \{p, q\} \in \{x, y, z\}$ :

$$W_1^2 + W_2^2 + W_3^2 + W_4^2 + W_5^2 + W_6^2 + W_7^2 + W_8^2 = 2W_0^2 \quad (20)$$

The above suggests that the equivalent 3D degree of polarization can be defined as:

$$m^{(3D)} = \frac{\sqrt{W_1^2 + W_2^2 + W_3^2 + W_4^2 + W_5^2 + W_6^2 + W_7^2 + W_8^2}}{\sqrt{2}W_0} \quad (21)$$

As can be seen, the current formalism provides the capability of a 3D transformation of EM field observables (e.g., vectors (16)–(17)) that is the appropriate way for translating or expressing a 3D EM field scattering phenomenon into various frames of reference (e.g., coordinate system). Upon performing the desired transformation, the

above field vectors can be re-gauged to radiation gauge, i.e., zero longitudinal return [13]. This gauge is the basis for the conventional polarimetric remote sensing  $h, v$  formalism. One should note that the dimension of these field vectors must be conserved, even if the elements are zero.

For a 3D unitary transformation “ $\mathbf{U}$ ”, the scattering matrix is defined by:

$$\mathbf{S}_U^{(3D)} = \mathbf{U}\mathbf{S}^{(3D)}\mathbf{U}^T \quad (22)$$

The required transformation for the scattering target vector (16) is given by:

$$k_{UGM} = \overline{\overline{\mathbf{U}}}k_{GM} \quad (23)$$

and for the Stokes vector (17) by:

$$\overline{\overline{\mathbf{G}}}_{(3D)}^U = \overline{\overline{\mathbf{U}}}\overline{\overline{\mathbf{G}}}_{(3D)} \quad (24)$$

The equivalent 3D transformation in (23)–(24) is defined by:

$$\overline{\overline{\mathbf{U}}} = A^{(3D)}\mathbf{U} \otimes \mathbf{U}A^{(3D)\dagger} \quad (25)$$

In (25),  $\overline{\overline{\mathbf{U}}}$  is a  $(9 \times 9)$  matrix transformation, and  $\otimes$  denotes the Kronecker product. Similarly, one can express the transformation for the scattering vector in (4) as:

$$\overline{\overline{\mathbf{S}}}_U^{(3D)} = T\overline{\overline{\mathbf{S}}}^{(3D)} \quad (26)$$

where

$$T = \mathbf{U} \otimes \mathbf{U} \quad (27)$$

An example for transformation  $\mathbf{U}$  is a 3D rotation that can be described by using Dupin convention and coordinate system [14] as:

$$\mathbf{U} = \mathbf{R}(\varphi, \theta) = \begin{bmatrix} \cos(\varphi) & -\sin(\varphi) & 0 \\ \cos(\theta)\sin(\varphi) & \cos(\theta)\cos(\varphi) & -\sin(\theta) \\ \sin(\theta)\sin(\varphi) & \sin(\theta)\cos(\varphi) & \cos(\theta) \end{bmatrix} \quad (28)$$

where  $\varphi$  and  $\theta$  represent the aspect and elevation rotation angles. The coordinate transformation or rotation in (26), i.e.,  $(\hat{\mathbf{x}}, \hat{\mathbf{y}}, \hat{\mathbf{z}} \rightarrow \hat{\mathbf{x}}', \hat{\mathbf{y}}', \hat{\mathbf{z}}')$  is depicted in Figure 1. One should note that, according to Dupin convention, choice of transversal components (surface unit vectors) is not unique, i.e., the normal vector rotation  $(\hat{\mathbf{z}} \rightarrow \hat{\mathbf{z}}')$  can be uniquely defined but choice of  $(\hat{\mathbf{x}}', \hat{\mathbf{y}}')$  is not unique.

Consider the conventional Stokes vector in 2D defined by:

$$\overline{\overline{\mathbf{G}}} = \begin{bmatrix} \langle |E_x|^2 \rangle + \langle |E_y|^2 \rangle \\ \langle |E_x|^2 \rangle - \langle |E_y|^2 \rangle \\ \langle E_x E_y^* \rangle + \langle E_y E_x^* \rangle \\ -j(\langle E_x E_y^* \rangle - \langle E_y E_x^* \rangle) \end{bmatrix} = \begin{bmatrix} G_0 \\ G_1 \\ G_2 \\ G_3 \end{bmatrix} \quad (29)$$

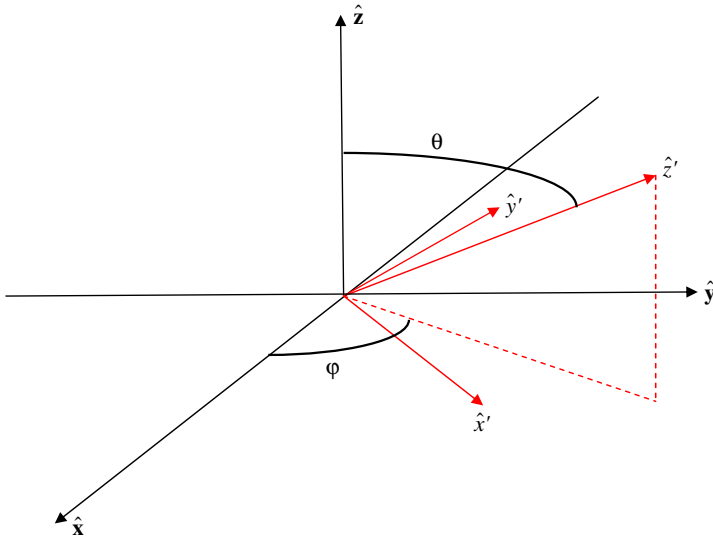


**Figure 1.** A 3-dimensional coordinate rotation example ( $\hat{\mathbf{z}}' = \mathbf{R}^T(\varphi, \theta)\hat{\mathbf{z}}$ ).

with degree of polarization:

$$m = \frac{\sqrt{G_1^2 + G_2^2 + G_3^2}}{G_0} \tag{30}$$

Assuming a transversal polarization, i.e.,  $E_z = 0$ , the 3D Stokes vector reads as:

$$\overline{\overline{\mathbf{G}}}_{(3D)} = \frac{1}{\sqrt{2}} \begin{bmatrix} \frac{\sqrt{6}}{3}G_0 & G_1 & \frac{\sqrt{3}}{3}G_0 & G_2 & 0 & 0 & G_3 & 0 & 0 \end{bmatrix}^t \tag{31}$$

Hence, the relation between the 2D and 3D degrees of polarization ((21) and (30)) can be written as:

$$\left(m^{(3D)}\right)^2 = \frac{3}{4} \left(m^2 + \frac{1}{3}\right) \tag{32}$$

Equation (32) shows that a fully-polarized EM wave in 2D is fully polarized in 3D. For a completely depolarized waveform in 2D, however, a degree of polarization of 0.5 is obtained in 3D. This non-zero degree of polarization in 3D can be attributed to the fact that although transversal components of the EM waveform are depolarized, the transversally polarized assumption introduces a constraint, and therefore, a certain degree of polarization in a 3D context.

#### 4. IMPLICATIONS FOR COMPACT POLARIMETRY

Compact polarimetry (CP) offers effective exploitation of SAR partial polarimetry (e.g., dual-pol) through scattered EM field analysis [15–18]. Although all the advantageous features of full polarimetry (full-quadrature) are not available, CP introduces performance improvement compared to conventional dual-pol applications.

Stokes vector and parameters are convenient for multiplatform applications as knowledge of the coherent source or illumination is not needed for their definitions. The described parameters, however, are reference-frame dependent. The latter implies that comparison or association of 2D Stokes parameters defined in different reference field planes (i.e.,  $[EH]$  plane) becomes ambiguous. The required mechanism for a proper transformation and association of the Stokes vector components is provided by the current Stokes formalism due to its 3D nature. The procedure for properly transforming the Stokes vector components between platforms can be detailed as following:

- 1- Calculate 2D Stokes vector  $\overline{\overline{G}}$  from (29) ( $x \rightarrow h, y \rightarrow v$ ),
- 2- Calculate 3D Stokes vector  $\overline{\overline{G}}_{(3D)}$  from (31),
- 3- Calculate the transformed (to an assumed unique reference base) 3D Stokes vector  $\overline{\overline{G}}_{(3D)}^U$  using (24)–(25),
- 4- Calculate the transformed/re-gauged 2D Stokes vector using:

$$\overline{\overline{G}}_{2D}^U = \sqrt{2} \begin{bmatrix} \frac{3}{\sqrt{6}} \overline{\overline{G}}_{3D}^U(1) \\ \overline{\overline{G}}_{3D}^U(2) \\ \overline{\overline{G}}_{3D}^U(4) \\ \overline{\overline{G}}_{3D}^U(7) \end{bmatrix} \quad (33)$$

Step 3 is important for unifying the Stokes vector definitions from multiple platforms. As will be discussed, accurate multi-platform polarimetric SAR data and product association within a unified reference frame results in enhanced target exploitation. It is shown (see Appendix) that Stokes and scattering vector transformation (25) is unitary for unitary 3D base transformations. Examples for these 3D base transformations (3D rotations) are given by (28). Such unitary nature results in norm-invariance of the 3D Stokes and scattering vectors. This is, however, not true for 2D vectors undergoing a 3D transformation.

### 5. BISTATIC CONSIDERATIONS

In a backscattering (monostatic) scenario, transmit and receive directions are aligned, i.e., transmit and receive wave fields are in the same  $[\mathbf{EH}]$  plane constructed by unit vectors  $(\hat{\mathbf{h}}, \hat{\mathbf{v}})$ . LOS unit vector is defined by the cross product  $\hat{\mathbf{l}} = \hat{\mathbf{h}} \times \hat{\mathbf{v}}$ . In 2D, the scattering matrix (see Appendix) elements represent co-pol and cross-pol reflections. The 3D extension of this backscattering case was presented in the last section.

For a bistatic scenario, transmit and receive directions are not aligned. This highlights other aspects of target scattering and nature for exploitations, albeit with the cost of more analytic complexity. In this case, the incident or transmit wave field is in a plane identified by unit vectors  $(\hat{\mathbf{h}}_i, \hat{\mathbf{v}}_i)$  and normal (i.e., LOS or alignment) vector  $\hat{\mathbf{l}}_i = \hat{\mathbf{h}}_i \times \hat{\mathbf{v}}_i$ . The scattered or observation wave field is in a plane identified by unit vectors  $(\hat{\mathbf{h}}_s, \hat{\mathbf{v}}_s)$  and normal vector  $\hat{\mathbf{l}}_s = \hat{\mathbf{h}}_s \times \hat{\mathbf{v}}_s$ . The angle between  $\hat{\mathbf{l}}_i$  and  $\hat{\mathbf{l}}_s$  determine the bistatic baseline. For a 2D bistatic scenario, the scattering matrix elements represent the co-pol and cross-pol reflections in a bistatic context, i.e., the diagonal elements represent  $S_{h_s h_i}, S_{v_s v_i}$  and the cross terms represent  $S_{h_s v_i}, S_{v_s h_i}$ . Although different in scattering nature from physics point of view, any 2D bistatic scattering matrix ( $2 \times 2$  complex matrix) can still be mathematically decomposed into complete set of Pauli spin base matrices. Decomposition, however, would have bistatic significance rather the conventional backscattering interpretation (e.g., trihedral associated with  $\sigma_0$  projection). For instance, the term associated with  $\sigma_0$  (i.e.,  $S_{h_s h_i} + S_{v_s v_i}$ ) would present co-pol reflection in a bistatic sense, that is along the  $(\hat{\mathbf{l}}_i, \hat{\mathbf{l}}_s)$  baseline. According to the above, exploitation and transformations must be tailored for bistatic scattering. The current 3D extension for bistatic scattering can be formulated as following.

$$\text{For a bistatic case } \mathbf{S}_{\mathbf{l}_s \mathbf{l}_i}^{(3D)} = \begin{bmatrix} S_{h_s h_i} & S_{h_s v_i} & S_{h_s l_i} \\ S_{v_s h_i} & S_{v_s v_i} & S_{v_s l_i} \\ S_{l_s h_i} & S_{l_s v_i} & S_{l_s l_i} \end{bmatrix}, \text{ the 3D}$$

scattering vector can be written as:

$$\tilde{\mathbf{S}}_{\mathbf{l}_s \mathbf{l}_i}^{(3D)} = (S_{h_s h_i} \ S_{h_s v_i} \ S_{h_s l_i} \ S_{v_s h_i} \ S_{v_s v_i} \ S_{v_s l_i} \ S_{l_s h_i} \ S_{l_s v_i} \ S_{l_s l_i})^t \quad (34)$$

As discussed earlier, 3D bistatic scattering matrix ( $3 \times 3$  complex matrix) can be mathematically decomposed into complete set of Gell-Mann base matrices (6)–(14).

In Gell-Mann basis, the scattering 9-vector becomes:

$$k_{GM}^{bi} = \frac{1}{\sqrt{2}} \begin{bmatrix} \frac{\sqrt{6}}{3} (S_{h_s h_i} + S_{v_s v_i} + S_{l_s l_i}) \\ S_{h_s h_i} - S_{v_s v_i} \\ \frac{\sqrt{3}}{3} (S_{h_s h_i} + S_{v_s v_i} - 2S_{l_s l_i}) \\ S_{h_s v_i} + S_{v_s h_i} \\ S_{h_s l_i} + S_{l_s h_i} \\ S_{v_s l_i} + S_{l_s v_i} \\ -j(S_{h_s v_i} - S_{v_s h_i}) \\ -j(S_{h_s l_i} - S_{l_s h_i}) \\ -j(S_{v_s l_i} - S_{l_s v_i}) \end{bmatrix} \quad (35)$$

3D transformation of bistatic scattering 9-vector (34)–(35) is more complicated due to both incident and scattered or transmit and receive transformation requirement, i.e., right and left operators. The 3D-transformed bistatic matrix can be defined by:

$$\mathbf{S}_{W_{1s} \mathbf{l}_i}^{(3D)} = \mathbf{W}_s \mathbf{S}_{\mathbf{l}_s \mathbf{l}_i}^{(3D)} \mathbf{W}_i^T \quad (36)$$

where  $\mathbf{W}_i$  and  $\mathbf{W}_s$  represent the transmit and receive 3D base transformations, respectively. For backscattering,  $\mathbf{W}_i = \mathbf{W}_s = \mathbf{U}$ , as described in (22).

The required transformation for bistatic scattering vector (35) is:

$$k_{GM}^{Wbi} = \overline{\overline{W}} k_{GM}^{bi} \quad (37)$$

with

$$\overline{\overline{W}} = A^{(3D)} \mathbf{W}_s \otimes \mathbf{W}_i A^{(3D)\dagger} \quad (38)$$

For the scattered wave Stokes vector, one gets:

$$\overline{\overline{G}}_{(3D)}^{Wbi} = \overline{\overline{W}}_s \overline{\overline{G}}_{(3D)}^{bi} \quad (39)$$

$$\overline{\overline{W}}_s = A^{(3D)} \mathbf{W}_s \otimes \mathbf{W}_s A^{(3D)\dagger} \quad (40)$$

The formalism detailed in this and previous sections provide the tool for 3D transformation of general scattering, i.e., back and bistatic scattering.

## 6. PRACTICAL APPLICATIONS

### 6.1. Multi-platform Unambiguous Polarimetric SAR Exploitations

Accurate association or combination of multi-platform SAR polarimetric products can be made possible within a 3D framework. The

transformed 3D scattering vectors from each platform to the reference frame are:

$$\bar{S}_{io}^{(3D)} = T_{io} \bar{S}_i^{(3D)} \quad (41)$$

where  $\bar{S}_i^{(3D)}$  is the 3D scattering vector observed at platform  $i$  and  $T_{io}$  represents 3D transformation between platform  $i$  and reference frame, as given by (27). The same description applies for scattering vectors in the Gell-Mann basis  $k_{GMi}$  and Stokes vector  $\bar{G}_{(3D)}^i$  where the appropriate platform to reference frame transformations  $\bar{U}_{io}$  given by (25) are used:

$$k_{GMio} = \bar{U}_{io} k_{GMi} \quad (42)$$

$$\bar{G}_{(3D)}^{io} = \bar{U}_{io} \bar{G}_{(3D)}^i \quad (43)$$

The set of reference frame 3D observables  $\bar{S}_{io}^{(3D)}$ ,  $k_{GMio}$  and  $\bar{G}_{(3D)}^{io}$  (with or without 2D re-gauging) can be used for consistent multi-platform SAR target analysis. The reference frame expression of 3D polarimetric products also offers possibility of superposing such products for multi-platform collaborative target exploitations. This fusion is especially suitable for permanent scatterer analysis. Introduce:

$$\bar{S}_o^{(3D)} = \sum_i \bar{S}_{io}^{(3D)} \quad (44)$$

$$k_{GMo} = \sum_i k_{GMio} \quad (45)$$

$$\bar{G}_{(3D)}^o = \sum_i \bar{G}_{(3D)}^{io} \quad (46)$$

3D polarimetric scattering products in (44)–(46) can be used for target characterization upon developing 3D characterization schemes. However, as mentioned, one can also re-gauge  $\bar{S}_o^{(3D)}$ ,  $k_{GMo}$  and  $\bar{G}_{(3D)}^o$  products to 2D for conventional polarimetric target analysis and classification. The 2D re-gauging is essentially maintaining the upper  $2 \times 2$  sub-matrix of the 3D scattering matrix ( $3 \times 3$ ) upon 3D transformations. For the 9-vector, this is equivalent to keep  $\bar{S}_1^{(3D)}$ ,  $\bar{S}_2^{(3D)}$ ,  $\bar{S}_4^{(3D)}$ ,  $\bar{S}_5^{(3D)}$  and set the rest to zero. It is also straightforward to transform the above superposed products to an arbitrary reference frame (using the associated 3D transformations (25) or (27)) for target analysis. The reason for the latter is the possibility of better manifestation of target characteristics in a certain reference frame LOS

(for 2D re-gauging, in particular). The described procedure can be summarized as follows:

- 1) Define 3D polarimetric products for each SAR platform  $i$ , i.e., apply (4), (16)–(17) when the longitudinal ( $z$ ) component set to zero.
- 2) Use 3D transformations in (25) and (27) for transformation to reference frame and derive  $\bar{S}_{io}^{(3D)}$ ,  $k_{GMio}$  or  $\bar{G}_{(3D)}^{io}$ . Since the same reference is used by all platforms, the required transformation (28) can be directly defined by SAR product look and incident angles. These derived vectors are in general 3D and have non-zero longitudinal ( $z$ ) components.
- 3) If required, derive the superposed products given by (44)–(46).

Following example can illustrate an application of the described procedure for multi-platform polarimetric SAR data/product harmonization and unification. Two fully polarimetric RADARSAT-2 (C-band, fine quad-pol FQ6/15) complex images are selected for analysis. Figure 2 depicts the quad-pol images acquired over Shirley's Bay (west of Ottawa, Canada) on September 23 and November 24, 2008. The images are chosen not to be a so-called coherent pair for the purpose of emulating multi-platform image acquisition, i.e., different look and incident angles. Coherent pair is typically referred to images acquired at the same SAR sensor location (i.e., temporally multiples of SAR orbit cycle, 24 days for RADARSAT-2) for coherent exploitations, e.g., change detection/monitoring. This, however, does not mean pairs collected otherwise may not be exploited coherently (e.g., interferometry, coherent stereos). In the RGB map depicted in Figure 2, red, green and blue represent  $HH$  ( $S_{hh}$ ),  $VV$  ( $S_{vv}$ ), and  $HV$  ( $S_{hv}$ ) channels, respectively. Figure 3 shows Pauli decompositions of a common chip (approximate) extracted from the two images and processed in Matlab. In these RGB images, red, green and blue represent double-bounce, volumetric, and single-bounce/surface backscattering mechanisms, respectively. As indicated in Figures 2 and 3, polarimetric channels and decomposition components are defined in the associated reference frames that have different basis vector sets, i.e., different  $h$ ,  $v$  definitions. Target decomposition components (Pauli) for the two images are transformed to the same reference frame based on steps 1 and 2 detailed above, re-gauged to 2D and included in Figure 4. The two decomposition maps are now defined within the same reference frame and can be accurately associated for enhanced target characterization, e.g., fusion. As can be seen from Figures 3 and 4, there is certain change of scattering mechanism distribution associated with transformation to another frame. Also, degree of this change (Figure 5) is

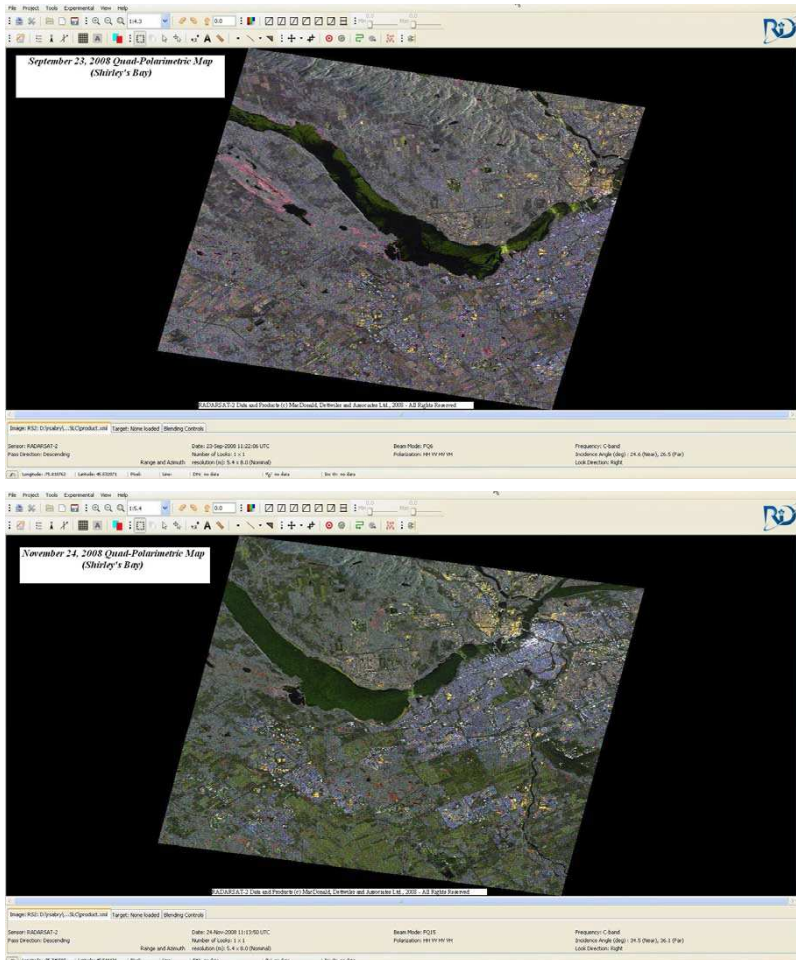


**Figure 2.** September 23 and November 24, 2008 quad-polarimetric images of Shirley's Bay with nominal range and azimuth resolutions of 5.4 and 8.0 meters (RGB:  $R = HH$ ,  $G = VV$ ,  $B = HV$ ); September 23: Look Angle =  $102.2^\circ$  (W.R.TN), Incident Angle =  $24.6^\circ$ – $26.5^\circ$  (Near-Far); November 24: Look Angle =  $100.7^\circ$  (W.R.TN), Incident Angle =  $34.5^\circ$ – $36.1^\circ$  (Near-Far).

different for the two scenarios considering the difference between their original imaging geometry (i.e., look and incident angles). Important outcome is that target decomposition components are now characterizing the same target backscattering property. Since scattering characteristics change during the temporal baseline (a month for this case),

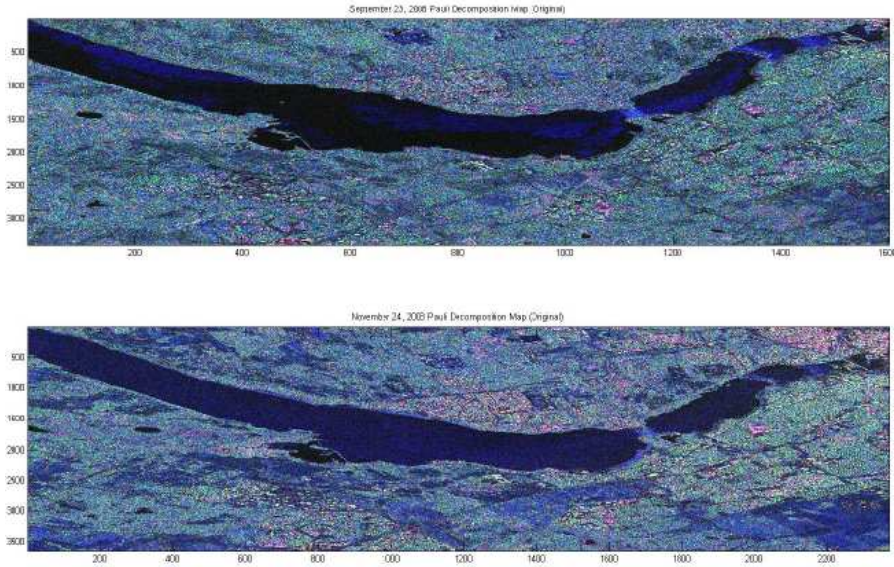


**Figure 3.** Original (prior to transformation) Pauli decomposition maps of September 23 and November 24, 2008 quad-pol imagery; RGB:  $R = \|HH - VV\|$  (double-bounce),  $G = \|HV\|$  (volume),  $B = \|HH + VV\|$  (single-bounce/surface). Decomposition maps have different basis.

backscattering specifications of a target observed in Figure 4 maps do not necessarily match, even when perfectly co-registered. For permanent scatterers, however, a better match should be expected.

One should note the following in regards to the introduced example and Figures 3–4. An effort has been made to extract a common chip from the two images for manipulation in Matlab. However, although images are georeferenced, accurate pixel-based co-registration of processed images is not possible due to difference in respective original slant plane (different incident and look angles) data processing. Visual inspection of the images (Figure 2) supports this by indicating the difference in range-azimuth alignments that results in different rectangular pixel formation. As hinted, the rectangular (as opposed to square) pixel formation of RADARSAT-2 imagery (i.e., different range and azimuth resolutions) adds to difficulty. Accordingly, the extracted complex Matlab images cannot exactly correspond on pixel basis. Nonetheless, the example provides an intuitive understanding of the process and value gained. Furthermore, as addressed, future multi-platform SAR data acquisition capabilities, tailored data processing and registration can address such issues.

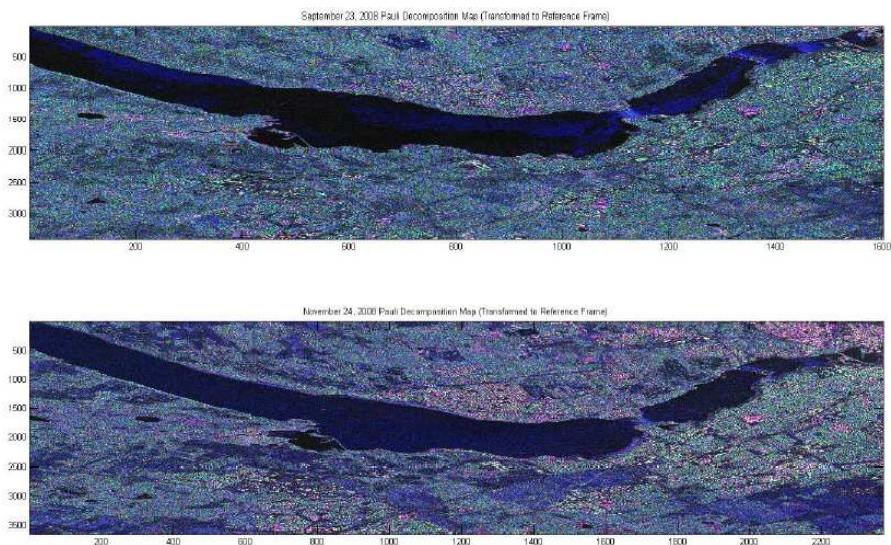


**Figure 4.** Transformed (to the reference frame) Pauli decomposition maps of September 23 and November 24, 2008 quad-pol imagery; RGB:  $R = \|HH - VV\|$  (double-bounce),  $G = \|HV\|$  (volume),  $B = \|HH + VV\|$  (single-bounce/surface). Both decomposition maps have the same basis.

## 6.2. 3-Dimensional Feature Extraction

The 3D target scattering products (i.e., 9-vector) described by (4), (16)–(17) provide means for 3D target scattering analysis. This 3D analysis is needed when 3D EM modeling is required, e.g., 3D scattering, multi-platform/multi-LOS SAR scattering analysis. As hinted earlier, however, 3D characterization schemes need to be developed that are not currently available in the literature. One also notes that, similar to 2D feature extraction (e.g., Pauli decomposition), 3D feature extraction of complex SAR image and association with a well-defined scattering mechanism for target or object may not be straightforward at the pixel level. Here, the objective is not to develop these schemes which represents a considerable challenge. Nevertheless, it is required and this work intends to initiate such endeavours. Considering the advances in EM computations and theory applications, the required modeling in 3D should not be insurmountable.

The 3D scattering decomposition is the extension of 2D decomposition. Although analogy to 2D is not always easy to draw, there should be 3D scattering significance to associated 3D components

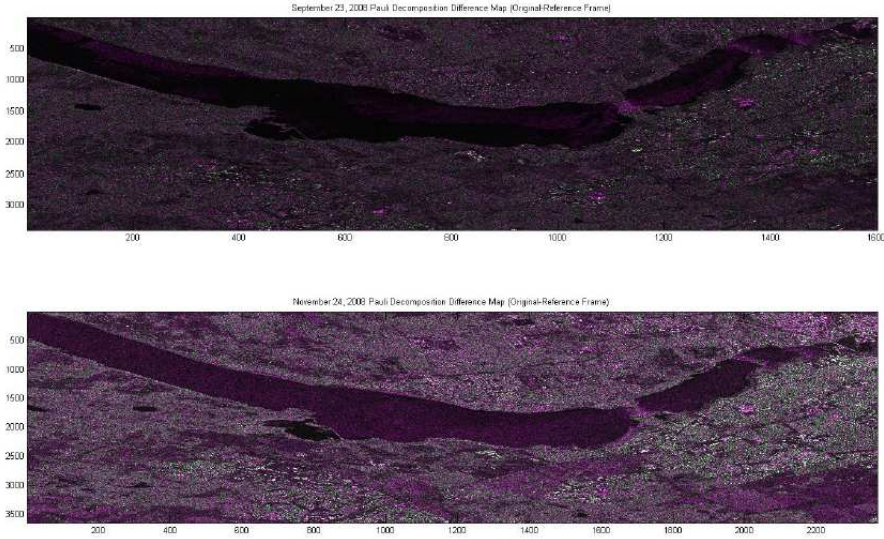


**Figure 5.** Pauli decomposition difference maps (Original-Reference Frame) for September 23 and November 24, 2008 quad-pol imagery; RGB:  $R = \|\Delta(HH - VV)\|$  (double-bounce),  $G = \|\Delta HV\|$  (volume),  $B = \|\Delta(HH + VV)\|$  (single-bounce/surface),  $\Delta \equiv$  original – transformed.

if the mathematical framework is consistent. For example, the first Pauli spin matrix  $\sigma_0$  represents odd bounce or trihedral scattering that is typically viewed as a point source for calibration. The first component of the scattering vector in the Gell-Mann basis  $k_{GM}$  that associates with  $\beta_9^{(c)}$  given by (14) can be viewed as a 3D point source representing scattering isometry. This can be used for calibration or scattering interpretation of 3D objects. Similarly, the second component that associates with  $\beta_3$  given by (8), models a dihedral lying in the transversal plane. Similar interpretations can be found for all  $9k_{GM}$  components. Thus, one can view the scattering vector in the Gell-Mann basis  $k_{GM}$  as a more comprehensive or generalized 3D Pauli decomposition that is standard for conventional polarimetric analysis. Procedure for this 3D (i.e., 9-vector) decomposition and transformation to different reference frames, has been detailed here.

## 7. SUMMARY AND CONCLUSIONS

A 3D formalism is in general important when the 3D field characterization is required. The introduced 3D framework for manipulation of multi-platform radar observables offers a leverage

to avoid ambiguities caused by observation-based  $h$ ,  $v$  definitions (coordinates and polarization). Upcoming multi-sensor multistatic missions (e.g., RCM, RS2) will require more systematic and universal handling of SAR polarimetric data. A 3D polarimetric data structure is beneficial to target data decomposition and exploitation.

The 3D Stokes formalism is mathematically convenient and robust for CP applications and analysis. This is due to the self-consistent nature of the 3D formalism, which allows unambiguous and/or universal definition of field observables defined in multiplatform reference frames, i.e., lines of sight. The 3D equivalent-to-Stokes vector is invariant under a unitary 3D transformation that is the proper coordinate transformation for any realistic scattering scenario.

Applicability of present formalism is discussed and theoretically explored based on the current and future multi-polarimetric SAR data exploitation requirements and objectives. The introduced coherent scattering vector definition in the Gell-Mann basis (i.e., generalization of the well-known Pauli target decomposition) provides a robust 3D base decomposition for comprehensive target scattering modeling. It is discussed that the 9-vector Gell-Mann components represent 3D scattering mechanisms analogous to those of Pauli 2D mechanisms.

Meaningful experimental validation and simulation of the proposed technique using polarimetric SAR imagery require certain 3D capability and multi-platform/multi-SAR coherent data (e.g., synchronization, co-registration) that is not currently available. The objective is to initiate such data acquisition in the community for enhanced exploitations. Some recent and developing missions, e.g., TanDEM-X (TerraSAR-X twin satellites), RCM, are very promising to provide accurate data and imagery for intended validations and real scenario applications.

## APPENDIX A. WAVE ENERGY CONSERVATION

In order to validate the 3D wave energy conservation, one needs to show the transformation  $\overline{\overline{\mathbf{U}}}$  in (25) is unitary, i.e.,  $\overline{\overline{\mathbf{U}}}\overline{\overline{\mathbf{U}}}^\dagger = I_9$ , where  $I_9$  is a  $(9 \times 9)$  identity matrix. According to Equation (25) and taking into account the unitary similarity nature of  $A^{(3D)}$ , i.e.,  $A^{(3D)}A^{(3D)\dagger} = I_9$ :

$$\begin{aligned} \overline{\overline{\mathbf{U}}}\overline{\overline{\mathbf{U}}}^\dagger &= \left( A^{(3D)}\mathbf{U} \otimes \mathbf{U}A^{(3D)\dagger} \right) \left( A^{(3D)}\mathbf{U} \otimes \mathbf{U}A^{(3D)\dagger} \right)^\dagger \\ &= \left( A^{(3D)} \right) (\mathbf{U} \otimes \mathbf{U}) \left( A^{(3D)\dagger} A^{(3D)} \right) (\mathbf{U} \otimes \mathbf{U})^\dagger \left( A^{(3D)\dagger} \right) \\ &= \left( A^{(3D)} \right) (\mathbf{U} \otimes \mathbf{U}) (\mathbf{U} \otimes \mathbf{U})^\dagger \left( A^{(3D)\dagger} \right) \end{aligned} \quad (A1)$$

Taking advantage of the following operator identities:

$$(\mathbf{X} \otimes \mathbf{Y})^\dagger = \mathbf{X}^\dagger \otimes \mathbf{Y}^\dagger \quad (\text{A2})$$

$$(\mathbf{V} \otimes \mathbf{W})(\mathbf{X} \otimes \mathbf{Y}) = (\mathbf{V}\mathbf{X}) \otimes (\mathbf{W}\mathbf{Y}) \quad (\text{A3})$$

one obtains:

$$(\mathbf{U} \otimes \mathbf{U})(\mathbf{U} \otimes \mathbf{U})^\dagger = (\mathbf{U}\mathbf{U}^\dagger) \otimes (\mathbf{U}\mathbf{U}^\dagger) = I_3 \otimes I_3 = I_9 \quad (\text{A4})$$

Thus, (A1) becomes:

$$\overline{\overline{\mathbf{U}}\mathbf{U}^\dagger} = A^{(3D)}I_9A^{(3D)\dagger} = I_9 \quad (\text{A5})$$

that verifies the energy conservation.

Identity (A3) can be proven by considering the core general operator relation for the  $n \times n$  matrix vectorization:

$$V^{(n)}(\mathbf{A}_{n \times n} \mathbf{Y}_{n \times n} \mathbf{B}_{n \times n}) = (\mathbf{A}_{n \times n} \otimes \mathbf{B}_{n \times n}^T) V^{(n)}(\mathbf{Y}_{n \times n}) \quad (\text{A6})$$

Consider (dropping the matrix/vector indices) the  $n^2$  — vector  $V(\mathbf{A} \mathbf{B} \mathbf{Y} \mathbf{C} \mathbf{D})$ .

Using (A6):

$$\begin{aligned} V(\mathbf{A} \mathbf{B} \mathbf{Y} \mathbf{C} \mathbf{D}) &= V((\mathbf{A} \mathbf{B}) \mathbf{Y} (\mathbf{C} \mathbf{D})) = ((\mathbf{A} \mathbf{B}) \otimes (\mathbf{C} \mathbf{D})^T) V(\mathbf{Y}) \\ &= ((\mathbf{A} \mathbf{B}) \otimes (\mathbf{D}^T \mathbf{C}^T)) V(\mathbf{Y}) \end{aligned} \quad (\text{A7})$$

On the other hand, applying (A6) gives:

$$\begin{aligned} V(\mathbf{A} \mathbf{B} \mathbf{Y} \mathbf{C} \mathbf{D}) &= V(\mathbf{A} (\mathbf{B} \mathbf{Y} \mathbf{C}) \mathbf{D}) = (\mathbf{A} \otimes \mathbf{D}^T) V(\mathbf{B} \mathbf{Y} \mathbf{C}) \\ &= (\mathbf{A} \otimes \mathbf{D}^T) (\mathbf{B} \otimes \mathbf{C}^T) V(\mathbf{Y}) \end{aligned} \quad (\text{A8})$$

Applying (A7) and (A8) for every  $\mathbf{Y}$ , one can obtain (A3).

## REFERENCES

1. Cloude, S. R. and E. Pottier, "A review of target decomposition theorems in radar polarimetry," *IEEE Trans. Geosci. Remote Sens.*, Vol. 34, No. 2, 498–518, Mar. 1996.
2. Cloude, S. R. and E. Pottier, "An entropy based classification scheme for land applications of polarimetric SARs," *IEEE Trans. Geosci. Remote Sens.*, Vol. 35, No. 1, 68–78, Jan. 1997.
3. Lee, J. S., M. R. Grunes, T. L. Ainsworth, L. Du, D. L. Schuler, and S. R. Cloude, "Unsupervised classification of polarimetric SAR images by applying target decomposition and complex Wishart distribution," *IEEE Trans. Geosci. Remote Sens.*, Vol. 37, No. 5, 2249–2258, Sep. 1999.

4. Pottier, E. and J. S. Lee, "Application of the H/A/ $\alpha$  polarimetric decomposition theorem for unsupervised classification of fully polarimetric SAR data based on the Wishart distribution," *Proc. CEOS Workshop*, 335–340, Toulouse, France, Oct. 26–29, 1999.
5. Cameron, W. L., N. Youssef, and L. K. Leung, "Simulated polarimetric signatures of primitive geometrical shapes," *IEEE Trans. Geosci. Remote Sens.*, Vol. 34, No. 3, 793–803, May 1996.
6. Cameron, W. L. and H. Rais, "Conservative polarimetric scatterers and their role in incorrect extensions of the Cameron decomposition," *IEEE Trans. Geosci. Remote Sens.*, Vol. 44, No. 12, 3506–3516, Dec. 2006.
7. Cameron, W. L. and H. Rais, "Polarization symmetric scatterer metric space," *IEEE Trans. Geosci. Remote Sens.*, Vol. 47, No. 4, 1097–1107, Apr. 2009.
8. Touzi, R. and F. Charbonneau, "Characterization of target symmetric scattering using polarimetric SARs," *IEEE Trans. Geosci. Remote Sens.*, Vol. 40, No. 11, 2507–2516, Nov. 2002.
9. Touzi, R., "Target scattering decomposition in terms of roll-invariant target parameters," *IEEE Trans. Geosci. Remote Sens.*, Vol. 45, No. 1, 73–84, Jan. 2007.
10. Touzi, R., A. Deschamps, and G. Rother, "Phase of target scattering for wetland characterization using polarimetric C-band SAR," *IEEE Trans. Geosci. Remote Sens.*, Vol. 47, No. 9, 3241–3261, Sep. 2009.
11. Vyplavin, P. I., K. A. Lukin, and N. N. Kolchigin, "Imaging with a noise SAR in the near-field of the source," *Telecommunications and Radio Engineering*, Vol. 66, No. 17, 1521–1531, 2007.
12. Cloude, S. R., "Lie groups in electromagnetic wave propagation and scattering," *Journal of Electromagnetic Waves and Applications*, Vol. 6, No. 7, 947–974, 1992.
13. Schwinger, J., *Classical Electrodynamics*, Perseus Books, MA, 1998.
14. Tai, C. T., *Generalized Vector and Dyadic Analysis*, IEEE Press, 1992.
15. Raney, R. K., "Hybrid-polarity SAR architecture," *IEEE Trans. Geosci. Remote Sens.*, Vol. 45, No. 11, 3397–3404, Nov. 2007.
16. Raney, R. K., "Dual-polarized SAR and Stokes parameters," *IEEE Geosci. Remote Sens. Lett.*, Vol. 3, No. 3, 317–319, Jul. 2006.
17. Souyris, J.-C. and S. Mingot, "Polarimetry based on one transmitting and two receiving polarizations: The  $\pi/4$  mode,"

- Proc. IGARSS*, 629–631, Toronto, ON, Canada, Jun. 24–28, 2002.
18. Souyris, J.-C., P. Imbo, R. Fjortoft, S. Mingot, and J.-S. Lee, “Compact polarimetry based on symmetry properties of geophysical media: The  $\pi/4$  mode,” *IEEE Trans. Geosci. Remote Sens.*, Vol. 43, No. 3, 634–646, Mar. 2005.
  19. Collin, R. E., *Antennas and Radiowave Propagation*, McGraw-Hill, 1985.
  20. Bell, D. C. and R. M. Naryanan, “Theoretical aspects of radar imaging using stochastic waveforms,” *IEEE Trans. on Signal Processing*, Vol. 49, No. 2, 394–400, 2001.
  21. Theron, I. P., E. K. Walton, and S. Gunawan, “Compact range radar cross-section measurements using a noise radar,” *IEEE Trans. Antennas Propagat.*, Vol. 46, 1285–1288, 1998.
  22. Jakowatz, C. V., et al., *Spotlight-Mode Synthetic Aperture Radar: A Signal Processing Approach*, Kluwer, 1996.